

XTSFormer: Cross-Temporal-Scale Transformer for Irregular Time Event Prediction

Tingsong Xiao¹, Zelin Xu¹, Wenchong He¹, Jim Su¹, Yupu Zhang¹, Raymond Opoku²,
Ronald Ison², Jason Petho², Jiang Bian², Patrick Tighe², Parisa Rashidi³, Zhe Jiang¹

¹Department of Computer & Information Science & Engineering, University of Florida, Gainesville, FL

²UF Health, Gainesville, FL

³Department of Biomedical Engineering, University of Florida, Gainesville, FL

{xiaotingsong, zelin.xu, whe2, jimsu, y.zhang1, raymond.opoku, rison, bianjiang, zhe.jiang}@ufl.com,
jpet0001@shands.ufl.edu, ptighe@anest.ufl.edu, parisa.rashidi@bme.ufl.edu

Abstract

Event prediction aims to forecast the time and type of a future event based on a historical event sequence. Despite its significance, several challenges exist, including the irregularity of time intervals between consecutive events, the existence of cycles, periodicity, and multi-scale event interactions, as well as the high computational costs for long event sequences. Existing neural temporal point processes (TPPs) methods do not capture the multi-scale nature of event interactions, which is common in many real-world applications such as clinical event data. To address these issues, we propose the cross-temporal-scale transformer (XTSFormer), designed specifically for irregularly timed event data. Our model comprises two vital components: a novel Feature-based Cycle-aware Time Positional Encoding (FCPE) that adeptly captures the cyclical nature of time, and a hierarchical multi-scale temporal attention mechanism. These scales are determined by a bottom-up clustering algorithm. Extensive experiments on several real-world datasets show that our XTSFormer outperforms several baseline methods in prediction performance.

ical operation patterns can identify anomalous or potentially erroneous clinical operations deviating from clinical practice guidelines before they occur, e.g., forgetting a certain medication or lab order by mistake. The learned event patterns can also facilitate generating real-world evidence through retrospective analysis of EHRs to help design improvement of clinical operations in medical practice. Figure 1 presents an illustrative example, where the event sequence represents a patient’s medication intake. In this sequence, medication type 1 is taken nearly every 12 hours, and medication type 2 is taken about every two days. This scenario exhibits multi-scale and cyclic patterns commonly observed in healthcare event data.

However, this domain presents several challenges. First, the irregularity of time intervals between events makes common time series prediction methods insufficient. Second, the event sequence patterns exhibit cycles, periodicity, and the multi-scale effect. For example, clinical operational events such as medication administration in operating rooms occur on a fine scale, typically within minutes. Conversely, events pre- or post-operation are on a coarser scale, often spanning hours or days. Similarly, in the realm of consumer behavior, purchasing frequency markedly rises during festivals compared to normal days, which see less frequent buying activities. Both scenarios exemplify the multi-scale nature of events in different contexts. However, accurately modeling these complex patterns, especially within extended event sequences, can involve high computational costs.

1 Introduction

Given a sequence of historical events with timestamps and types, event prediction aims to predict the time and type of the next event. This problem is common in many application domains, such as user behavior modeling in recommender systems [Wang *et al.*, 2021], fraud detection in financial transactions [Bacry *et al.*, 2015], and disease modeling based on electronic health records (EHRs) [Liu *et al.*, 2022b]. In the health domain, adverse events related to unsafe care are among the top ten causes of death in the U.S. [Dingley *et al.*, 2011]. The large volume of EHR data being collected in hospitals, together with recent advancements in machine learning and artificial intelligence, provide unique opportunities for data-driven and evidence-based clinical decision-making systems. Event prediction by learning common clin-

ical operation patterns can identify anomalous or potentially erroneous clinical operations deviating from clinical practice guidelines before they occur, e.g., forgetting a certain medication or lab order by mistake. The learned event patterns can also facilitate generating real-world evidence through retrospective analysis of EHRs to help design improvement of clinical operations in medical practice. Figure 1 presents an illustrative example, where the event sequence represents a patient’s medication intake. In this sequence, medication type 1 is taken nearly every 12 hours, and medication type 2 is taken about every two days. This scenario exhibits multi-scale and cyclic patterns commonly observed in healthcare event data.

However, this domain presents several challenges. First, the irregularity of time intervals between events makes common time series prediction methods insufficient. Second, the event sequence patterns exhibit cycles, periodicity, and the multi-scale effect. For example, clinical operational events such as medication administration in operating rooms occur on a fine scale, typically within minutes. Conversely, events pre- or post-operation are on a coarser scale, often spanning hours or days. Similarly, in the realm of consumer behavior, purchasing frequency markedly rises during festivals compared to normal days, which see less frequent buying activities. Both scenarios exemplify the multi-scale nature of events in different contexts. However, accurately modeling these complex patterns, especially within extended event sequences, can involve high computational costs.

Existing methods are generally based on the temporal point processes (TPPs), a common framework for modeling asynchronous event sequences in continuous time [Cox and Isham, 1980; Schoenberg *et al.*, 2002]. Traditional statistical TPPs models [Daley and Vere-Jones, 2008] characterize the stochastic nature of event timing but can only capture simple patterns in event occurrences such as self-excitation [Hawkes, 1971]. More recently, deep learning methods (also called neural TPPs) have become more popular due to the capability of modeling complex event dependencies in the intensity function of TPPs. Recurrent neural networks (RNNs), known for their inherent ability to process sequential data, were first introduced to neural TPPs, with models like Recurrent Marked Temporal Point Process (RMTTPP) [Du *et al.*, 2016],

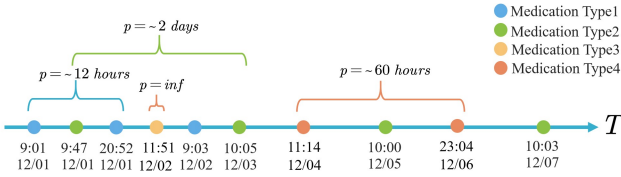


Figure 1: An example of medication taken sequence in EHRs.

continuous-time LSTM (CT-LSTM) [Mei and Eisner, 2017], and Intensity Function-based models [Xiao *et al.*, 2017; Omi *et al.*, 2019]. While LSTM-based approaches address some challenges like vanishing gradients, other issues such as long-range dependencies remain unresolved. Transformers [Vaswani *et al.*, 2017], leveraging their self-attention mechanism, circumvent the long-range dependency problem by allowing direct interactions between all events in a sequence. For example, Transformer Hawkes Process (THP) [Zuo *et al.*, 2020] leverages the self-attention mechanism to efficiently capture long-term dependencies across varied event sequence data. Meanwhile, the Self-Attentive Hawkes Process (SAHP) [Zhang *et al.*, 2020] employs the translation of time intervals into phase shifts of sinusoidal functions, coupled with self-attention, as a strategy for enhanced feature learning. Moreover, [Yang *et al.*, 2022] enhances the neural Hawkes process [Mei and Eisner, 2017] by replacing its architecture with a flatter attention-based model. However, these methods do not capture the important multi-scale patterns within event sequences. There are some works on multi-scale transformers (e.g., Scaleformer [Shabani *et al.*, 2023] and Pyraformer [Liu *et al.*, 2022a]) and efficient transformers (e.g., LogTrans [Li *et al.*, 2019] and Informer [Zhou *et al.*, 2021]) for time series data, but these methods assume regular time intervals and thus are not applicable for irregular time event prediction.

To address these challenges, we propose a novel cross-temporal-scale transformer (XTSFormer) for irregular time event prediction. Our XTSFormer consists of feature-based cycle-aware time positional encoding and cross-scale attention within a multi-scale time hierarchy. Specifically, we define the time scale on irregular time event sequences by the merging order of a bottom-up clustering algorithm (e.g., agglomerative). The intuition is that events with shorter intervals (at smaller scales) will be merged earlier. We designed a cross-scale attention operation by specifying the key set as nodes in the same scale level. In summary, we make the following contributions.

- To the best of our knowledge, XTSFormer is a pioneering work in neural Temporal Point Processes (TPPs), integrating multi-scale features that are crucial for practical applications like clinical event analysis.
- The model introduces two theoretical advancements: the Feature-based Cycle-aware Positional Encoding to enhance the capture of complex temporal patterns by incorporating both feature and cyclical information, and a cross-scale attention mechanism that improves time efficiency compared to the standard all-pair attention.
- Experiments on two public datasets and two real patient

safety datasets demonstrate the superior performance of our proposed XTSformer. We present a detailed evaluation that shows our model outperforms established benchmarks, thereby validating the effectiveness of our methodological contributions.

2 Related Work

2.1 Neural Temporal Point Process

Beyond RNNs-based and Transformer-based TPP models that we discussed in the introduction, various neural TPP models have emerged with diverse methodologies. Works such as [Eom *et al.*, 2022; Li *et al.*, 2020] employ inference and logic rules to model latent variables, aiming to understand sequence features. [Lin *et al.*, 2022] introduces GNTPP, a deep generative approach, to create high-quality time samples. [Bae *et al.*, 2022] brings a new perspective by utilizing a meta-learning framework to represent TPPs as neural processes. Meanwhile, [Zhang *et al.*, 2021] formulates a latent graph to emphasize the influence of significant event types, [Wang *et al.*, 2023] introduces a novel regularizer for maximum likelihood estimation using a hierarchical contrastive learning approach, and [Zhou *et al.*, 2023] innovatively uses convolutional kernels to merge both local and global contexts. Moreover, there are several neural ODE-based methods for TPPs. Since the neural ODE cannot be directly applied to discrete event sequences (as the events do not occur at every time point in the continuous time domain, unlike the temperature variable), a stochastic process on jumps between discrete events to enhance the neural ODE framework is utilized [Jia and Benson, 2019; Chen *et al.*, 2020]. Lastly, [Zhang *et al.*, 2022] explores the modeling of distributions via a Dirichlet distribution specifically for event sequence clustering. Collectively, these studies demonstrate the rich diversity and continued evolution of neural TPP modeling techniques.

2.2 Cluster-based Transformer and Multi-scale Temporal Attention

Cluster-based Transformers like [Vyas *et al.*, 2020; Wang *et al.*, 2022] conducted clustering in the latent token embeddings (latent feature space) while lacking in the time domain to capture the multiple temporal scale patterns. There are several multi-scale temporal attention but most of them focus on the regular domain. For example, [Hu *et al.*, 2022] employs multi-scale temporal correlations to identify high and low-frequency actions in a regular time series context. [Dai *et al.*, 2022] is also tailored for regular time series data, where actions within a video follow a regular temporal pattern. Both of these methods are not suitable for irregular situations.

2.3 Positional Encoding

Positional encoding is crucial in Transformer-based models, capturing the relative order of events in TPPs. Two primary kinds of positional encoding are prevalent: fixed and learned. Fixed encoding, such as the one used in [Vaswani *et al.*, 2017], computes absolute positional encoding by applying order numbers to sinusoidal functions. Learned encoding, on the other hand, can be subdivided into two main cat-

egories that either consider periodic cycles or not. Examples of the former include [Kazemi *et al.*, 2019; Xu *et al.*, 2020; Zhang *et al.*, 2020; Xu *et al.*, 2019], which use sinusoidal functions to model time’s cyclical nature, and [Li *et al.*, 2021], which offers a learnable Fourier feature mapping for multi-dimensional encoding. Among them, the multi-recurrent cycle-aware encoding [Dikeoulas *et al.*, 2022] decomposes time into multiple fixed cycles like months, weeks, and days to capture recurring temporal patterns, which is not sufficient for applications where cycles are not well-defined. The latter category, including [Shaw *et al.*, 2018; Raffel *et al.*, 2020], aims to learn the representation of relative position, with [Liu *et al.*, 2020] proposing a neural ordinary differential equation (ODE) approach and [Wang *et al.*, 2019] introducing a structural method that blends both absolute and relative positional encoding strategies.

3 Methodology

Consider a temporal sequence \mathcal{Q} of events denoted as $\langle e_1, \dots, e_i, \dots, e_L \rangle$, where L represents the sequence length. Each event, e_i , can be characterized by a pair (t_i, k_i) : t_i signifies the event time, and $k_i \in \{1, 2, \dots, n_K\}$ indicates the event type, with K denoting the total number of type classes. The objective of the event prediction problem is to predict the subsequent event, $e_{L+1} = (t_{L+1}, k_{L+1})$. It’s important to note that the time of each event, t_i , is irregular, i.e., events don’t occur at fixed intervals. These event times can exhibit patterns across various temporal scales. To illustrate, clinical operational events like medication administration may be recorded at minute intervals within an operation room, yet they might be logged hourly when noted pre- or post-operation.

3.1 Overall model architecture

This section introduces our proposed cross-temporal-scale transformer (XTSFormer) model, as illustrated in Figure 2. The model consists of two parts: (a) construction of a hierarchical tree, feature-based cycle-aware time positional encoding, and cross-temporal-scale module (encoder); (b) event time and type prediction (decoder). Our main idea is to establish a multi-scale time hierarchy and conduct cross-scale attention with selective key sets in each scale. Latent features are processed using pooling operations across multiple scale levels.

3.2 Feature-based Cycle-aware Time Positional Encoding

To effectively capture complex cyclic patterns in irregular time sequences, we introduce a novel Feature-based Cycle-aware Time Positional Encoding (FCPE). Traditional temporal positional encoding primarily focuses on encoding continuous timestamps. However, research has shown that incorporating semantic features is vital for accurately representing periodic patterns in various real-world phenomena [Ke *et al.*, 2021; Zhang *et al.*, 2019]. FCPE is designed to address this by integrating these crucial semantic aspects into the encoding of time intervals between events.

Time positional encoding can be described as a function $\mathcal{P} : T \rightarrow \mathbb{R}^{d \times 1}$, mapping from the time domain $T \subset \mathbb{R}$

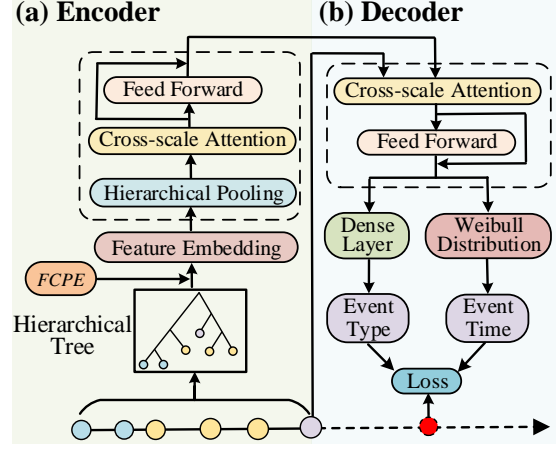


Figure 2: The flowchart of the proposed XTSFormer.

to a d -dimensional vector space. In attention mechanisms, it is the dot product of time positional encodings that matter [Xu *et al.*, 2019]. Therefore, the relative timespan $|t_a - t_b|$ between events a and b implies crucial temporal information, where t_a and t_b represent the time points of occurrence for events a and b , respectively. Considering events a and b , we define a temporal kernel $\mathcal{K} : T \times T \rightarrow \mathbb{R}$, such that

$$\mathcal{K}(t_a, t_b) = \mathcal{P}(t_a) \cdot \mathcal{P}(t_b) = \mathcal{F}(t_a - t_b), \quad (1)$$

where \mathcal{F} is a location invariant function of the timespan. As proofed in **Appendix 1.1**, the kernel \mathcal{K} defined above satisfies the assumptions of Bochner’s Theorem, as stated below:

Theorem 1 (Bochner’s Theorem). *A continuous, translation-invariant kernel $\mathcal{K}(t_a, t_b) = \mathcal{F}(t_a - t_b)$ is positive definite if and only if there exists a non-negative measure on \mathbb{R} such that \mathcal{F} is the Fourier transform of the measure.*

Given this, the kernel \mathcal{K} can be represented as Eq. (2):

$$\mathcal{F}(t_a - t_b) = \int_{-\infty}^{\infty} e^{iw(t_a - t_b)} p(w) dw. \quad (2)$$

Different from [Xu *et al.*, 2020], which uses the Monte Carlo integral [Rahimi and Recht, 2007] to approximate the expectation of \mathcal{F} , we sample the probability density $p(w_k)$ on several frequencies w_k and learn $p(w_k)$ based on the event feature, where $k = 0, \dots, \frac{d}{2} - 1$ (d is an even integer). The frequencies w_k are learnable parameters initialized as $\frac{2\pi k}{d}$, corresponding to the Discrete Fourier Transform (DFT) of the spectral density function, as follows.

$$\mathcal{F}(t_a - t_b) \approx \sum_{k=1}^{\frac{d}{2}} \mu(k) e^{iw_k(t_a - t_b)} = \sum_{k=1}^{\frac{d}{2}} \mu^k \cos(w_k(t_a - t_b)), \quad (3)$$

where $\mu(k)$ (representing $p(w_k)$) is the non-negative power spectrum at the frequency index k and $\frac{d}{2}$ denotes the number of frequencies. Considering that w_k is learnable, μ^k is the learned probability density corresponding to frequency w_k .

Thus following the above conditions and to satisfy Eq. (1) and Eq. (3), we propose the final positional encoding function $\mathcal{P}(t_i)$ for time t_i as shown in Eq. (4), where d is the encoding dimension, w_k is the k -th sample of frequency, and μ_i^k is the learned feature-based probability density corresponding to w_k . Specifically, $\mu_i = [\mu_i^1, \mu_i^2, \dots, \mu_i^{\frac{d}{2}}]^T$ can be expressed as $\mu_i = W^\mu \mathbf{k}_i$, where $W^\mu \in \mathbb{R}^{\frac{d}{2} \times K}$ is a learnable parameter matrix for feature-based probability density μ_i , and $\mathbf{k}_i \in \mathbb{R}^{K \times 1}$ is the one-hot encoding of event type k_i .

$$\mathcal{P}(t_i) = \begin{bmatrix} \mu_i^1 \cos(w_1 t_i) \\ \mu_i^1 \sin(w_1 t_i) \\ \mu_i^2 \cos(w_2 t_i) \\ \mu_i^2 \sin(w_2 t_i) \\ \vdots \\ \mu_i^{\frac{d}{2}} \cos(w_{\frac{d}{2}} t_i) \\ \mu_i^{\frac{d}{2}} \sin(w_{\frac{d}{2}} t_i) \end{bmatrix} \in \mathbb{R}^{d \times 1} \quad (4)$$

The advantages of our FCPE are twofold. First, it builds upon the assumption that any point in time can be represented as a vector derived from a series of sine and cosine functions that reflect the cyclical nature of time with varying intensities and frequencies, which is suitable for modeling irregular time intervals. Second, we propose learning the intensities associated with each sample frequency based on the event semantic features (e.g., event type) at a particular time. Ideally, event types that occur frequently will be reflected in higher density values μ^k on the higher frequency w_k . As shown in **Appendix 1.2**, FCPE’s translation invariance ensures stability, sustaining performance even when there are shifts in the input feature.

Following the temporal positional encoding $\mathcal{P}(t_i)$, we merged it with a non-temporal feature representation, i.e., $f_i = W^k \mathbf{k}_i + \mathcal{P}(t_i)$, where f_i is the entire embedding i -th event, and $W^k \in \mathbb{R}^{d \times K}$ is a learnable parameter matrix for non-temporal embedding.

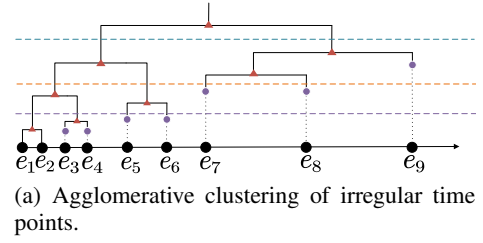
3.3 Cross-temporal-scale Module on Irregular Event Sequence

The cross-temporal-scale module consists of hierarchical pooling and cross-scale attention as shown in Figure 2(a).

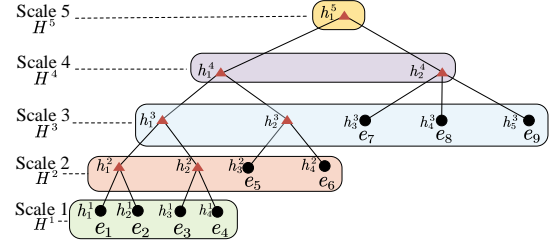
One unique challenge of designing cross-scale attention on irregular time event sequences is that there is no obvious definition of temporal scales. This is different from regular time series data, where different temporal scales can be easily defined based on the original or downsampled resolutions. For irregular time event sequences, intuitively, events that occur with short time intervals tend to interact with each other at a small time scale (e.g., medications every few minutes within the operation room), while events with longer intervals are at a large time scale (e.g., medication every few days post-operation). Here we would like to establish the temporal scale concept on irregular time sequences in an algorithmic manner. We do this by hierarchical clustering.

Hierarchical pooling layer

We define the temporal scales on irregular time points through a bottom-up hierarchical clustering, e.g., agglomerative [Day



(a) Agglomerative clustering of irregular time points.



(b) Scale hierarchy based on merging order.

Figure 3: An illustration of multi-scale hierarchy on irregular time points by bottom-up clustering.

and Edelsbrunner, 1984]. The agglomerative algorithm starts with each time point as an initial cluster and recursively merges the two closest clusters each time (measured by the minimum, maximum, or centroid distance among point pairs) until all intermediate clusters are merged into one. The greedy criteria used in the agglomeration algorithm enforce that time points that are closer to each other (in smaller scales) be merged earlier. Therefore, we can determine the temporal scale based on the cluster merging order in a multi-level hierarchy. Figure 3 illustrates this process with an example. There are nine events e_1 to e_9 . Figure 3(a) shows the bottom-up clustering process with one merging operation at a time. The merging order of intermediate clusters is shown by the levels of vertical bars. In this example, points e_1 to e_2 are merged first, then e_3 and e_4 , followed by e_5 and e_6 . Next, two leftmost intermediate clusters are merged. The process continues until all clusters are merged into a root node. The merging order indicates that e_7 and e_8 are at a larger time scale than e_1 and e_2 . This is consistent with our intuition when looking at the point distribution.

To quantify the time scales of event points, we can vertically slice the merging order of all initial and intermediate clusters into different intervals. Those clusters that are merged in the s -th vertical interval from the bottom are in the scale of s . For example, in Figure 3(a), we can use three thresholds to split merging operations into four intervals. Within each interval, we can check the initial clusters before any merging in the interval and the final clusters before this interval ends. For example, e_1 and e_2 as well as e_3 and e_4 are merged into two internal nodes (red triangles) in the first (bottom) interval. Therefore, they are in scale 1. As another instance of example, e_7 , e_8 , and e_9 are merged in the third interval, and thus they are in scale 3. The cumulative merging process can be summarized in a hierarchical tree

structure like Figure 3(b), in which the **temporal scale** of a tree node can be defined by its level.

One important question is how to choose the slicing thresholds. The thresholds control the granularity of multiple scales. If we need fine-grained multi-scale levels, we need to set up a larger number of thresholds (intervals, or tree levels). In an extreme case, the total number of levels equals the number of event points. In practice, such a scale choice is likely inefficient. To control the number of (leaf or internal) points at each scale level, we can configure the slicing thresholds based on the number of merging operations. The multi-scale hierarchy in Figure 3(b) can be configured by setting the number of merging operations as 2, 2, 3, and 1 respectively. This will help us manage the number of intermediate clusters at each scale.

We denote the latent representations at different tree nodes in each scale level s as $H^s = [h_1^s, h_2^s, \dots, h_{n_s}^s]$, where h_j^s is the j -th node in scale s , and n_s is the number of nodes in scale s . Note that $h_j^s = f_j$ (raw embedding) for a leaf node (e_j) at the beginning. In Figure 3(b), there are four node representations in the 1st scale, four in the 2nd scale, and so on.

To aggregate the feature across different level scales, we conduct an average pooling operation (based on the tree hierarchy), and concatenation of pooled clusters with the clusters in the next scale.

Cross-scale attention layer

We now introduce our attention operation in the multi-scale time hierarchy. In the common all-pair attention, for each time point (query), we have to compute its attention weights to all points (keys). In our cross-scale temporal attention, for each tree node (query), we only do temporal attention on a selective key set, i.e., nodes in the same scale level. The cross-attention operation is expressed in Eq. (5), where \tilde{h}_j^s is the representation of h_j^s after cross-attention, q_j^s is the query vector for j th node at scale s , k_l^s is the key vector for the l -th node, v_l is the value vector, \mathcal{N}_j^s is the selective key set of h_j^s , and D_K is the dimension of key and query vectors as a normalizing term. Consider the example in Figure 3(b). The key set for e_6 (h_4^2) has four nodes (h_1^2 , h_2^2 , h_3^2 , and h_4^2), including itself. This reduces the total number of keys from 9 to 4.

$$\tilde{h}_j^s = \sum_{l \in \mathcal{N}_j^s} \frac{\exp(q_j^s k_l^{sT} / \sqrt{D_K}) v_l}{\sum_{l \in \mathcal{N}_j^s} \exp(q_j^s k_l^{sT} / \sqrt{D_K})}. \quad (5)$$

Iterative Process

Starting from the irregular time event sequence, we first do a bottom-up clustering to specify the multiple-scale hierarchy of event points. This is done in the preprocessing phase. Within the framework of our model, the procedure commences with embedding operations, encompassing both our FCPE and semantic feature embedding. Subsequently, the model progresses through the cross-temporal-scale module, from the smallest scale to the largest scale. At each scale, the model performs hierarchical pooling according to the tree hierarchy, cross-scale attention, and concatenates the pooled clusters with those in the subsequent scale. The iterations continue until they reach the root node. This process learns

complex multi-scale representation within a multi-level hierarchy without sacrificing granularity or specificity. Moreover, the approach enhances computational efficiency by reducing the size of a key set in cross-attention operations as shown in Figure 2(a).

Time cost analysis

The main advantages of the model include that it captures the multi-scale hierarchical patterns and more importantly that it can reduce attention operations. Assume the number of input temporal points is \hat{L} , batch size is B , number of heads is \hat{h} , and hidden dimension is \hat{d} . In our attention computation, the query matrix dimensions are represented by $Q \in \mathbb{R}^{B \times \hat{h} \times \hat{L} \times \hat{d}}$. For each query point Q_i (where $1 \leq i \leq \hat{L}$), its selective key set size is M (depending on the threshold in each level). Thus the key matrix results from concatenating key sets of all query points, yielding a dimension of $\mathbb{R}^{B \times \hat{h} \times \hat{L} \times M \times \hat{d}}$. Consequently, the Flops of the attention computation with our approach is $B \cdot \hat{h} \cdot \hat{L} \cdot M \cdot \hat{d}$, with the key set size M scaling $O(\log \hat{L})$. This results in significantly more efficient attention computation Flops, specifically $B \cdot \hat{h} \cdot \hat{L} \cdot \log \hat{L} \cdot \hat{d}$, compared to the vanilla transformer computation of $B \cdot \hat{h} \cdot \hat{L}^2 \cdot \hat{d}$.

3.4 Decoder and Loss Function

Our decoder comprises two parts: predicting event type and event time, as shown in Figure 2(b). Initially, we apply cross-scale attention at the topmost (largest) scale, using the last element as the query and the others as keys to encapsulate the temporal and sequential nature of the forthcoming event. Following this, we obtain H_L , the comprehensive latent representation of the entire past event sequence, by applying a dense layer to H^s . As H^s integrates features from multiple scales, it effectively discerns the temporal patterns of the incoming event.

Event type prediction

The prediction of the next event type, based on the latent embedding H_L of past events, is achieved through a dense transformation layer followed by a softmax function. This process generates the predicted probability distribution of the event type. We calculate the cross-entropy loss using the true event type labels and this predicted probability distribution, thus optimizing the model for accurate event type prediction.

Event time prediction

For predicting event time, we add another dense layer on top of H_L to learn the distribution parameters of the temporal point process, specifically the scale parameter λ and shape parameter γ . Unlike the typical use of an exponential distribution, we opt for the Weibull distribution [Rinne, 2008] to model the intensity function. The exponential distribution, a specific case of the Weibull distribution with $\gamma = 1$, has a constant intensity function suggesting events occur with a uniform likelihood, irrespective of past occurrences. This characteristic makes it less suitable for scenarios where historical events are influential. Conversely, the Weibull distribution, with its variable hazard function that can be increasing, decreasing, or constant, offers a flexible approach

Table 1: Results (average \pm std) of all methods on Medications and Providers dataset.

Methods	Medications				Providers			
	Accuracy (%)	F1-score (%)	RMSE	NLL	Accuracy (%)	F1-score (%)	RMSE	NLL
HP	21.9 \pm 1.1	18.1 \pm 2.1	2.78 \pm 0.33	3.54 \pm 0.38	32.1 \pm 2.5	31.9 \pm 2.6	5.17 \pm 1.30	2.19 \pm 0.13
RMTTP	23.4 \pm 0.6	20.1 \pm 1.8	1.87 \pm 0.77	3.10 \pm 0.18	35.7 \pm 2.1	33.2 \pm 2.7	4.11 \pm 1.40	2.23 \pm 0.11
CTLSTM	22.5 \pm 0.6	19.2 \pm 1.7	1.61 \pm 0.41	3.23 \pm 0.18	34.5 \pm 1.4	32.5 \pm 1.9	3.12 \pm 1.50	1.93 \pm 0.08
NJSDE	29.5 \pm 0.4	25.2 \pm 0.9	1.40 \pm 0.22	2.33 \pm 0.19	37.9 \pm 1.2	34.1 \pm 1.1	2.95 \pm 1.17	1.89 \pm 0.07
ODETPP	24.6 \pm 0.5	23.1 \pm 0.9	1.99 \pm 0.20	2.60 \pm 0.21	33.4 \pm 1.5	29.0 \pm 0.8	3.81 \pm 1.21	2.33 \pm 0.08
SAHP	28.4 \pm 0.9	25.5 \pm 2.1	1.81 \pm 0.30	2.44 \pm 0.21	38.0 \pm 1.9	37.2 \pm 2.1	3.55 \pm 1.93	2.10 \pm 0.09
THP	27.1 \pm 0.7	26.1 \pm 1.3	1.41 \pm 0.33	2.49 \pm 0.19	37.5 \pm 2.2	33.8 \pm 1.9	2.84 \pm 1.48	1.82 \pm 0.09
A-NHP	30.2 \pm 0.5	25.5 \pm 0.8	1.57 \pm 0.29	2.54 \pm 0.22	38.9 \pm 1.5	34.9 \pm 1.5	2.89 \pm 1.54	1.83 \pm 0.11
XTSFormer	33.5 \pm 0.8	29.4 \pm 1.1	1.12 \pm 0.24	2.23 \pm 0.20	43.9 \pm 1.3	37.2 \pm 1.5	2.33 \pm 1.74	1.75 \pm 0.10

to modeling how past events impact future probabilities. The comparative effectiveness of these two distributions as intensity functions is explored in the experimental section of our study.

We use the negative log-likelihood (NLL) of event time as the loss function for event time prediction:

$$\mathcal{L}_t = -\log P(t'; \lambda, \gamma) = -\log \left(\frac{\gamma}{\lambda} \left(\frac{t'}{\lambda} \right)^{\gamma-1} e^{-\left(\frac{t'}{\lambda} \right)^{\gamma}} \right), \quad (6)$$

where t' is the label time. The final loss is $\mathcal{L} = (1 - \alpha)\mathcal{L}_t + \alpha\mathcal{L}_p$, where α is a hyperparameter for trade-off.

4 Experimental Evaluation

The goal of the evaluation section is to compare our proposed XTSFormer with baseline models in neural TPPs in prediction performance (both event time and event type). We also demonstrate the importance of different components within our model through an ablation study. For the event type prediction task, we utilized the accuracy and the macro F1-score as evaluation metrics. Meanwhile, for the event time prediction task, the root mean square error (RMSE) and negative log-likelihood (NLL) were chosen as the performance metric. The detailed experimental setup is in **Appendix 2.1**.

4.1 Datasets and comparative methods

In the experiments, we utilized four datasets. These included two EHR datasets – Medications and Providers – sourced from our university hospital. Additionally, two public datasets were employed: Financial Transactions [Du *et al.*, 2016] and StackOverflow [Leskovec and Krevl, 2014]. A summary of these datasets is presented in **Appendix 2.2**.

The comparative baselines include one traditional algorithm, *i.e.*, Hawkes Processes (HP) [Zhang *et al.*, 2020], two RNN-based algorithms, *i.e.*, RMTTP [Du *et al.*, 2016] and CT-LSTM [Mei and Eisner, 2017], two ODE-based algorithms, *i.e.*, NJSDE [Jia and Benson, 2019] and ODETPP [Chen *et al.*, 2020], and three Transformer-based algorithms, *i.e.*, SAHP [Zhang *et al.*, 2020], THP [Zuo *et al.*, 2020], and A-NHP [Yang *et al.*, 2022].

4.2 Comparison on Prediction Performance

Table 1 summarizes the accuracy, F1-score, RMSE, and negative log-likelihood (NLL) of all evaluated methods on two datasets. Further experimental results on two additional datasets are detailed in **Appendix 2.3**. It is observed that the traditional HP model exhibits the lowest accuracy in predicting event types. The RNN-based models perform slightly better than HP in overall accuracy and F1-score. The Transformer-based models are generally more accurate than the RNN-based models. Their overall accuracy is around 4% to 5% higher than RNN-based models. Among transformer models, XTSFormer performs the best, whose overall accuracy is 3% to 5% higher than other transformers. This could be explained by the fact that our model captures the multi-scale temporal interactions among events. For event time prediction, we observe similar trends, except that the RMSE of event time prediction for SAHP is somehow worse than other transformers (close to the RNN-based models). The reason could be that the event sequences in our real-world datasets do not contain self-exciting patterns as assumed in the Hawkes process.

4.3 Ablation Study

To evaluate the effectiveness of our proposed model components, we conducted an ablation study on various datasets, including Medications, Providers, Financial, and StackOverflow. The study investigates the impact of FCPE, multi-scale temporal attention, and choice of event time distribution (Exponential or Weibull). Table 2 shows the RMSE results of the ablation study. Additional ablation study results are presented in **Appendix 2.4**. Specifically, we compare two kinds of positional encoding (PE), *i.e.*, traditional positional encoding (written as ‘base’) [Zuo *et al.*, 2020] and our FCPE. Moreover, we compare our model with (w/) and without (w/o) multi-scale parts. Meanwhile, we compare two kinds of distribution, *i.e.*, exponential distribution and Weibull distribution.

Base vs. FCPE. When transitioning from the base positional encoding to FCPE, we observe consistent performance improvements across all datasets. This highlights the effectiveness of FCPE in capturing the cyclic patterns and multi-scale temporal dependencies present in event sequences.

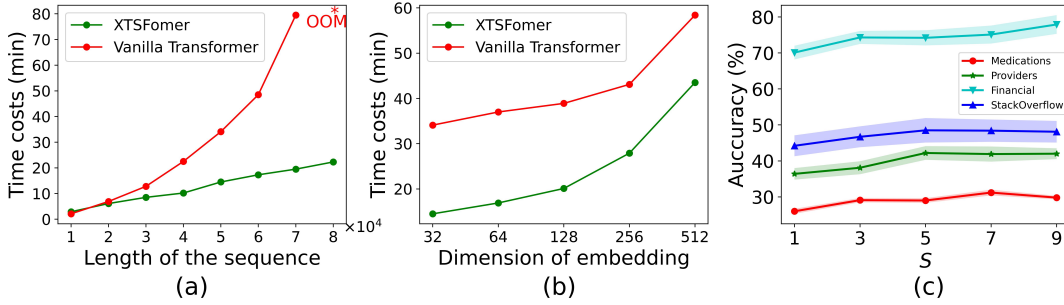


Figure 4: (a) is the time cost on different lengths of sequence (OOM indicates ‘out of memory’). (b) is the time cost of different dimensions of embeddings. (c) is the comparison of accuracy on various S scales.

Multi-scale attention. Introducing multi-scale attention further enhances predictive accuracy. The model with multi-scale attention consistently outperforms its counterpart without it. This demonstrates the significance of modeling interactions at different temporal scales, which is crucial for capturing complex event dependencies.

Exponential vs. Weibull. Comparing the two event time distributions, we find that the Weibull distribution yields better results. This aligns with our theoretical justification that the Weibull distribution can better reflect the varying influences of history on current events. The Weibull distribution, when incorporated into the point process, allows for capturing intricate temporal patterns influenced by past events, whereas the Exponential distribution remains memoryless.

Table 2: RMSE results of ablation study, where PE means positional encoding, MS means Multi-scale, Distrib. stands for Distribution, Med. stands for Medications, Prov. stands for Providers, Fin. stands for Financial, and SO stands for StackOverflow.

PE	MS	Distrib.	Med.	Prov.	Fin.	SO
base	w/o	Exponential	1.89	3.62	1.44	5.85
FCPE	w/o	Exponential	1.80	3.05	1.45	5.50
base	w/	Exponential	1.75	2.48	1.01	4.39
FCPE	w/	Exponential	1.15	2.40	0.92	4.22
base	w/o	Weibull	1.90	3.50	2.42	5.51
FCPE	w/o	Weibull	1.82	2.88	0.89	4.39
base	w/	Weibull	1.65	2.51	1.15	4.30
FCPE	w/	Weibull	1.12	2.33	0.88	4.21

4.4 Computational Time Costs

To evaluate the efficiency of our method on long event sequences, we have conducted computational experiments using a synthetic dataset as described in **Appendix 2.5**. This dataset comprises 64 event data sequences, each with a length of 100,000 events. In our experiments, we set the batch size $B = 1$ and the hidden dimension $d = 32$. We progressively increased the sequence length and recorded the time cost (in minutes). The results are shown in Figure 4(a). The time discrepancy between XTSFormer and Vanilla Transformer widens with increasing sequence length, underscoring the efficiency of the multi-scale approach.

Table 3: NLL results of ablation study, where PE means positional encoding, MS means Multi-scale, Distrib. stands for Distribution, Med. stands for Medications, Prov. stands for Providers, Fin. stands for Financial, and SO stands for StackOverflow.

PE	MS	Distrib.	Med.	Prov.	Fin.	SO
base	w/o	Exponential	3.48	2.21	2.10	2.88
FCPE	w/o	Exponential	2.99	2.15	2.07	2.41
base	w/	Exponential	2.47	1.92	1.60	2.42
FCPE	w/	Exponential	2.20	1.81	1.17	2.10
base	w/o	Weibull	2.59	2.30	2.35	2.31
FCPE	w/o	Weibull	2.34	2.10	2.11	2.09
base	w/	Weibull	2.31	1.89	1.59	2.02
FCPE	w/	Weibull	2.23	1.75	1.18	1.89

Furthermore, we conducted computational experiments on the different dimensions of embeddings, as shown in Figure 4(b). The Vanilla Transformer’s time costs increase significantly with larger embeddings, suggesting scalability issues. In contrast, XTSFormer scales more efficiently, maintaining lower time costs even at higher dimensions, making it a preferable option for tasks requiring large-scale data processing with limited computational resources.

4.5 Sensitivity Analysis

We investigate the parameter sensitivity by varying the largest scale $S \in \{1, 3, 5, 7, 9\}$ and report the accuracy results on four datasets in Figure 4(c). Notably, our method displays sensitivity to the largest scale S , as it determines the multi-scale intensity. For instance, when $S = 1$, only a single scale is present, leading to suboptimal performance.

5 Conclusion and Future Works

The paper proposed XTSFormer, a neural TPP model with feature-based cycle-aware time positional encoding and cross-scale temporal attention. Time scales are derived from a bottom-up clustering, prioritizing shorter interval events at smaller scales and the cross-scale attention mechanism assigns the key set as nodes at the same scale levels. The model’s effectiveness is validated through experiments on 4 real-world datasets. Future works will focus on robustness and reliability, particularly in outliers and noisy data scenarios.

References

- [Bacry *et al.*, 2015] Emmanuel Bacry, Iacopo Mastromatteo, and Jean-François Muzy. Hawkes processes in finance. *Market Microstructure and Liquidity*, 1(01):1550005, 2015.
- [Bae *et al.*, 2022] Wonho Bae, Mohamed Osama Ahmed, Frederick Tung, and Gabriel L Oliveira. Meta temporal point processes. In *The Eleventh International Conference on Learning Representations*, 2022.
- [Chen *et al.*, 2020] Ricky TQ Chen, Brandon Amos, and Maximilian Nickel. Neural spatio-temporal point processes. In *International Conference on Learning Representations*, 2020.
- [Cox and Isham, 1980] David Roxbee Cox and Valerie Isham. *Point processes*, volume 12. CRC Press, 1980.
- [Dai *et al.*, 2022] Rui Dai, Srijan Das, Kumara Kahatapitiya, Michael S Ryoo, and François Brémond. Ms-tct: multi-scale temporal convtransformer for action detection. In *Proceedings of the IEEE/CVF Conference on Computer Vision and Pattern Recognition*, pages 20041–20051, 2022.
- [Daley and Vere-Jones, 2008] Daryl J Daley and David Vere-Jones. *An introduction to the theory of point processes: volume II: general theory and structure*. Springer, 2008.
- [Day and Edelsbrunner, 1984] William HE Day and Herbert Edelsbrunner. Efficient algorithms for agglomerative hierarchical clustering methods. *Journal of classification*, 1:7–24, 1984.
- [Dikeoulis *et al.*, 2022] Ioannis Dikeoulis, Saadullah Amin, and Günter Neumann. Temporal knowledge graph reasoning with low-rank and model-agnostic representations. In *Proceedings of the 7th Workshop on Representation Learning for NLP*, pages 111–120, 2022.
- [Dingley *et al.*, 2011] Catherine Dingley, Kay Daugherty, Mary K Derieg, and Rebecca Persing. Improving patient safety through provider communication strategy enhancements. 2011.
- [Du *et al.*, 2016] Nan Du, Hanjun Dai, Rakshit Trivedi, Utkarsh Upadhyay, Manuel Gomez-Rodriguez, and Le Song. Recurrent marked temporal point processes: Embedding event history to vector. In *Proceedings of the 22nd ACM SIGKDD international conference on knowledge discovery and data mining*, pages 1555–1564, 2016.
- [Eom *et al.*, 2022] Deokjun Eom, Sehyun Lee, and Jaesik Choi. Variational neural temporal point process. *arXiv preprint arXiv:2202.10585*, 2022.
- [Hawkes, 1971] Alan G Hawkes. Point spectra of some mutually exciting point processes. *Journal of the Royal Statistical Society Series B: Statistical Methodology*, 33(3):438–443, 1971.
- [Hu *et al.*, 2022] Huazhang Hu, Sixun Dong, Yiqun Zhao, Dongze Lian, Zhengxin Li, and Shenghua Gao. Transrac: Encoding multi-scale temporal correlation with transformers for repetitive action counting. In *Proceedings of the IEEE/CVF Conference on Computer Vision and Pattern Recognition*, pages 19013–19022, 2022.
- [Jia and Benson, 2019] Junteng Jia and Austin R Benson. Neural jump stochastic differential equations. *Advances in Neural Information Processing Systems*, 32, 2019.
- [Kazemi *et al.*, 2019] Seyed Mehran Kazemi, Rishab Goel, Sepehr Eghbali, Janahan Ramanan, Jaspreet Sahota, Sanjay Thakur, Stella Wu, Cathal Smyth, Pascal Poupart, and Marcus Brubaker. Time2vec: Learning a vector representation of time. *arXiv preprint arXiv:1907.05321*, 2019.
- [Ke *et al.*, 2021] Guolin Ke, Di He, and Tie-Yan Liu. Re-thinking positional encoding in language pre-training. In *International Conference on Learning Representations*, 2021.
- [Leskovec and Krevl, 2014] Jure Leskovec and Andrej Krevl. Snap datasets: Stanford large network dataset collection, 2014.
- [Li *et al.*, 2019] Shiyang Li, Xiaoyong Jin, Yao Xuan, Xiyu Zhou, Wenhui Chen, Yu-Xiang Wang, and Xifeng Yan. Enhancing the locality and breaking the memory bottleneck of transformer on time series forecasting. *Advances in neural information processing systems*, 32, 2019.
- [Li *et al.*, 2020] Shuang Li, Lu Wang, Ruizhi Zhang, Xiaofu Chang, Xuqin Liu, Yao Xie, Yuan Qi, and Le Song. Temporal logic point processes. In *International Conference on Machine Learning*, pages 5990–6000. PMLR, 2020.
- [Li *et al.*, 2021] Yang Li, Si Si, Gang Li, Cho-Jui Hsieh, and Samy Bengio. Learnable fourier features for multi-dimensional spatial positional encoding. *Advances in Neural Information Processing Systems*, 34:15816–15829, 2021.
- [Lin *et al.*, 2022] Haitao Lin, Lirong Wu, Guojian Zhao, Liu Pai, and Stan Z Li. Exploring generative neural temporal point process. *Transactions on Machine Learning Research*, 2022.
- [Liu *et al.*, 2020] Xuanqing Liu, Hsiang-Fu Yu, Inderjit Dhillon, and Cho-Jui Hsieh. Learning to encode position for transformer with continuous dynamical model. In *International conference on machine learning*, pages 6327–6335. PMLR, 2020.
- [Liu *et al.*, 2022a] Shizhan Liu, Hang Yu, Cong Liao, Jianguo Li, Weiyao Lin, Alex X Liu, and Schahram Dustdar. Pyraformer: Low-complexity pyramidal attention for long-range time series modeling and forecasting. In *International Conference on Learning Representations*, 2022.
- [Liu *et al.*, 2022b] Sichen Liu, Xiaolong Wang, Yang Xiang, Hui Xu, Hui Wang, and Buzhou Tang. Multi-channel fusion lstm for medical event prediction using ehers. *Journal of Biomedical Informatics*, 127:104011, 2022.
- [Mei and Eisner, 2017] Hongyuan Mei and Jason M Eisner. The neural hawkes process: A neurally self-modulating multivariate point process. *Advances in neural information processing systems*, 30, 2017.
- [Omi *et al.*, 2019] Takahiro Omi, Kazuyuki Aihara, et al. Fully neural network based model for general temporal

- point processes. *Advances in neural information processing systems*, 32, 2019.
- [Raffel *et al.*, 2020] Colin Raffel, Noam Shazeer, Adam Roberts, Katherine Lee, Sharan Narang, Michael Matena, Yanqi Zhou, Wei Li, and Peter J Liu. Exploring the limits of transfer learning with a unified text-to-text transformer. *The Journal of Machine Learning Research*, 21(1):5485–5551, 2020.
- [Rahimi and Recht, 2007] Ali Rahimi and Benjamin Recht. Random features for large-scale kernel machines. *Advances in neural information processing systems*, 20, 2007.
- [Rinne, 2008] Horst Rinne. *The Weibull distribution: a handbook*. CRC press, 2008.
- [Schoenberg *et al.*, 2002] Frederic Paik Schoenberg, David R Brillinger, and PM Guttorp. Point processes, spatial-temporal. *Encyclopedia of environmetrics*, 3:1573–1577, 2002.
- [Shabani *et al.*, 2023] Amin Shabani, Amir Abdi, Lili Meng, and Tristan Sylvain. Scaleformer: Iterative multi-scale refining transformers for time series forecasting. In *International Conference on Learning Representations*, 2023.
- [Shaw *et al.*, 2018] Peter Shaw, Jakob Uszkoreit, and Ashish Vaswani. Self-attention with relative position representations. In *Proceedings of NAACL-HLT*, pages 464–468, 2018.
- [Vaswani *et al.*, 2017] Ashish Vaswani, Noam Shazeer, Niki Parmar, Jakob Uszkoreit, Llion Jones, Aidan N Gomez, Łukasz Kaiser, and Illia Polosukhin. Attention is all you need. *Advances in neural information processing systems*, 30, 2017.
- [Vyas *et al.*, 2020] Apoorv Vyas, Angelos Katharopoulos, and François Fleuret. Fast transformers with clustered attention. *Advances in Neural Information Processing Systems*, 33:21665–21674, 2020.
- [Wang *et al.*, 2019] Xing Wang, Zhaopeng Tu, Longyue Wang, and Shuming Shi. Self-attention with structural position representations. In *Proceedings of the 2019 Conference on Empirical Methods in Natural Language Processing and the 9th International Joint Conference on Natural Language Processing (EMNLP-IJCNLP)*. Association for Computational Linguistics, 2019.
- [Wang *et al.*, 2021] Dongjing Wang, Xin Zhang, Yao Wan, Dongjin Yu, Guandong Xu, and Shuiguang Deng. Modeling sequential listening behaviors with attentive temporal point process for next and next new music recommendation. *IEEE Transactions on Multimedia*, 24:4170–4182, 2021.
- [Wang *et al.*, 2022] Ningning Wang, Guobing Gan, Peng Zhang, Shuai Zhang, Junqiu Wei, Qun Liu, and Xin Jiang. Clusterformer: Neural clustering attention for efficient and effective transformer. In *Proceedings of the 60th Annual Meeting of the Association for Computational Linguistics (Volume 1: Long Papers)*, pages 2390–2402, 2022.
- [Wang *et al.*, 2023] Qingmei Wang, Minjie Cheng, Shen Yuan, and Hongteng Xu. Hierarchical contrastive learning for temporal point processes. *Proceedings of the AAAI Conference on Artificial Intelligence*, 37(8):10166–10174, Jun. 2023.
- [Xiao *et al.*, 2017] Shuai Xiao, Junchi Yan, Xiaokang Yang, Hongyuan Zha, and Stephen Chu. Modeling the intensity function of point process via recurrent neural networks. In *Proceedings of the AAAI conference on artificial intelligence*, volume 31, 2017.
- [Xu *et al.*, 2019] Da Xu, Chuanwei Ruan, Evren Korpeoglu, Sushant Kumar, and Kannan Achan. Self-attention with functional time representation learning. *Advances in neural information processing systems*, 32, 2019.
- [Xu *et al.*, 2020] Da Xu, chuanwei ruan, evren korpeoglu, sushant kumar, and kannan achan. Inductive representation learning on temporal graphs. In *International Conference on Learning Representations (ICLR)*, 2020.
- [Yang *et al.*, 2022] Chenghao Yang, Hongyuan Mei, and Jason Eisner. Transformer embeddings of irregularly spaced events and their participants. In *Proceedings of the Tenth International Conference on Learning Representations (ICLR)*, 2022.
- [Zhang *et al.*, 2019] Dongzhi Zhang, Kyungmi Lee, and Ick-jai Lee. Semantic periodic pattern mining from spatio-temporal trajectories. *Information Sciences*, 502:164–189, 2019.
- [Zhang *et al.*, 2020] Qiang Zhang, Aldo Lipani, Omer Kirnap, and Emine Yilmaz. Self-attentive hawkes process. In *International conference on machine learning*, pages 11183–11193. PMLR, 2020.
- [Zhang *et al.*, 2021] Qiang Zhang, Aldo Lipani, and Emine Yilmaz. Learning neural point processes with latent graphs. In *Proceedings of the Web Conference 2021*, pages 1495–1505, 2021.
- [Zhang *et al.*, 2022] Yunhao Zhang, Junchi Yan, Xiaolu Zhang, Jun Zhou, and Xiaokang Yang. Learning mixture of neural temporal point processes for multi-dimensional event sequence clustering. In *Proceedings of the Thirty-First International Joint Conference on Artificial Intelligence, Vienna, Austria*, pages 23–29, 2022.
- [Zhou *et al.*, 2021] Haoyi Zhou, Shanghang Zhang, Jieqi Peng, Shuai Zhang, Jianxin Li, Hui Xiong, and Wancai Zhang. Informer: Beyond efficient transformer for long sequence time-series forecasting. In *Proceedings of the AAAI conference on artificial intelligence*, volume 35, pages 11106–11115, 2021.
- [Zhou *et al.*, 2023] Wang-Tao Zhou, Zhao Kang, Ling Tian, and Yi Su. Intensity-free convolutional temporal point process: Incorporating local and global event contexts. *Information Sciences*, page 119318, 2023.
- [Zuo *et al.*, 2020] Simiao Zuo, Haoming Jiang, Zichong Li, Tuo Zhao, and Hongyuan Zha. Transformer hawkes process. In *International conference on machine learning*, pages 11692–11702. PMLR, 2020.